

### Influence of gaseous cavities in ship-hydrodynamic problems: a simplified study

G. Colicchio<sup>\*,\*\*</sup>      M. Greco<sup>\*,\*\*</sup>      O. M. Faltinsen<sup>\*\*</sup>  
g.colicchio@insean.it    m.greco@insean.it    oddfal@marin.ntnu.no

\* INSEAN, Italian Ship Model Basin, Roma – Italy.

\*\* Centre for Ships and Ocean Structures (CeSOS), NTNU, Trondheim – Norway.

Several phenomena of interest in ship hydrodynamics involve the presence of time-varying air cavities in the water flow. Two of the most well known, with important practical consequences, are the erosion of propeller blades and the noise. The former is connected with propellers working near the air-water interface and, in particular, to the formation of air cavities during cavitation events. It is caused by the propeller interaction with the air-water two-phase fluid and represents a danger for the success of the vessel operations. The latter is connected with entrapment of air cavities during breaking and fragmentation of the air-water interface. It is a consequence of the collapse of such bubbles evolving in the surrounding water and its major relevance is in military context. Cavitating bubbles are characterized by a uniform interior pressure equal to the vapor pressure. Instead, entrapped cavities have in principle a non uniform pressure. However, in many practical cases their inner pressure can be approximated as uniform with value generally time dependent, in particular compressibility may matter. Assuming a uniform pressure in the cavity means that the effect of the interior air flow on the surrounding water and structures is neglected.

The importance of air cavities entrapped during free-surface breaking has been investigated numerically by Colagrossi and Landrini (2003) in connection with the problem of a dam breaking followed by a water-wall impact. When the air was modeled inside a cavity entrapped after a wave breaking event, the pressure in the surrounding water and along the close structures changed substantially with respect to the case of a single-phase (water) simulation. Very high loads on breakwaters interacting with breaking waves were documented by Peregrine and Thaus (1996) and by Peregrine (2003) and explained through the compressibility of the cavities formed during the wave-structure impacts. The mentioned studies are of interest for sloshing and green-water events because the latter may involve liquid-liquid and liquid-structure impacts and so breaking of the gas-liquid interface and entrapment of cavities. In the context of water shipping, for instance, air entrainment was clearly observed during two- and three-dimensional model tests (see *i.e.* Greco *et al.* 2004 and Barcellona *et al.* 2003) and caused by water-vessel impacts and by air-water interface breaking.

Present study is a contribution to the investigation of air-cushion effects in ship-hydrodynamic problems. It represents the further development of the work by Colicchio and Greco (2006), with respect to which it models the splitting of a cavity in smaller ones and the merging of neighbor cavities into a single one. Numerical investigations of such phenomena were performed for instance by Caboussat *et al.* (2005) in connection with the filling of channels and by Rungsiyaphornat *et al.* (2003) in the case of underwater explosions.

Compressible cavities are modeled as follows: the effect of the interior gas flow on the surrounding fluid is neglected and the gas is assumed ideal and evolving according to the polytropic law

$$p_{cav} V_{cav}^\gamma = p_{cav0} V_{cav0}^\gamma, \quad (1)$$

$\gamma$  being the polytropic index.  $p_{cav}$  and  $V_{cav}$  are the pressure and volume of the cavity at the time  $t$ , respectively, and  $p_{cav0}$  and  $V_{cav0}$  represent the corresponding reference values, for instance those at the initial time (*i.e.* when the cavity was formed). The splitting of a cavity  $A$  with pressure  $p_A$  in  $N$  smaller bubbles is modeled assuming that the new cavities will have the same pressure as the cavity from where they are formed, that is

$$p_k = p_A \quad \text{for } k = 1..N \quad (2)$$

with  $k$  the generic cavity formed from the splitting. The volumes  $V_k$  are evaluated from the actual geometry and together with the pressures  $p_k$  give the initial conditions for the newly born cavities, *i.e.*  $p_{k0}$  and  $V_{k0}$ , from which the latter evolve in time according to law (1). The merging of  $N$  cavities into a single cavity  $A$  is modeled assuming that (i) the gas behaves still as ideal and (ii) the heat transfer from the involved bubbles to the liquid is negligible. The resulting conservation law is enforced by (iii) taking the volume of the new cavity as the sum of the volumes of the merging bubbles before their coalescence, that is

$$p_A V_A^\gamma = \left( \sum_{k=1}^{k=N} p_k V_k \right) \left( \sum_{k=1}^{k=N} V_k \right)^{\gamma-1} \quad (3)$$

with  $p_k$  and  $V_k$ , respectively, the pressure and volume of the generic cavity  $k$  involved in the merging process. Equation (3) gives the pressure  $p_A$  of the created cavity, once evaluated its volume  $V_A$  from the actual geometry.  $p_A$  and  $V_A$  represent the initial conditions for cavity  $A$ , *i.e.*  $p_{A0}$  and  $V_{A0}$ , and allow its further evolution according to law (1).

The simplified model developed for the air-cushion phenomenon has been introduced inside a 2D field method based on a Navier-Stokes (NS) solver. The latter uses a Projection scheme for the time integration and a finite difference scheme on a staggered grid for the spatial discretization, both correct to the second order. Further it is combined with a Level-Set (LS) technique to handle the deformation and breaking of the air-water interface (Colicchio *et al.* 2005). Within the solution algorithm, the pressure inside compressible cavities is considered known and given by one of the laws (1)-(2)-(3). The problem for the pressure and velocity fields involves the governing equation

$$H(\psi) \left[ \nabla \cdot \left( \frac{\nabla p}{\rho} + OT + \frac{(\mathbf{v} \cdot \nabla) \mathbf{v}}{\Delta t} \right) \right] + [1 - H(\psi)] (p - p_{cav}) = 0 \quad (4)$$

for the pressure  $p$ ,  $\rho$  being the fluid density,  $\mathbf{v}$  the fluid velocity,  $OT$  the viscous and surface-tension contributions and  $\Delta t$  the used time step. Further  $H(\psi)$  is a HeaviSide function that goes from 1 inside the liquid to 0 in the gas and depends on the signed distance  $\psi$  from their interface. Equation (4) coincides with the Poisson equation in the liquid and becomes a Dirichlet condition for the pressure inside a compressible cavity. The enforcement of this sharp change in the pressure conditions would lead to numerical problems in terms of robustness and stability. The same is true for the jump of the velocity across a liquid-gas interface caused by the approximation of zero flow within the gas cavity. To avoid such problems, the liquid velocity is extended for one cell and half inside a compressible bubble. This is made assuming that the velocity remains constant when crossing normally the interface. Further, in the numerical model, equation (4) is approximated as

$$H(\psi) \left[ \nabla \cdot \left( \frac{\nabla p}{\rho} + OT \right) \right] + \overline{H}(\psi) \frac{\nabla \cdot (\mathbf{v} \cdot \nabla) \mathbf{v}}{\Delta t} + \alpha [1 - \overline{H}(\psi)] (p - p_{cav}) = 0 \quad (5)$$

with  $\overline{H}$  a smoothed Heavy-Side function that limits the effects of the unphysical divergence contributions in the vicinity of compressible cavities and allows a gentle passage from a pressure equation to a pressure Dirichlet condition. Finally the coefficient  $\alpha = 1/\Delta x^4$  is used to improve the well-conditioning of the resulting algebraic system matrix. Consistently with the Level-Set technique, also  $\rho$  is smoothed across the gas-liquid interface. In connection with merging and collapse processes, a fundamental numerical challenge is the choice of the algorithm (i) for the search and affiliation of gas collocation points with the membership cavity, and (ii) for the prediction of merging/collapse phenomena.

The capability of the resulting numerical method in handling the evolution of compressible adiabatic cavities has been checked in Colicchio and Greco (2006) by studying the oscillations of an initially circular gas cavity surrounded by a ring of inviscid liquid with a constant external pressure. The analytical solution for small oscillation amplitudes relative to the bubble size was derived and the results for the oscillation period were compared with the one predicted numerically in steady-state regime. The agreement was globally satisfactory.

Here the merging modeling is investigated analyzing the problem of two initially circular air cavities surrounded by liquid inside a rectangular box 8 m long and 7 m high (see top-left sketch of figure 1). The cavities are subjected to the gravity

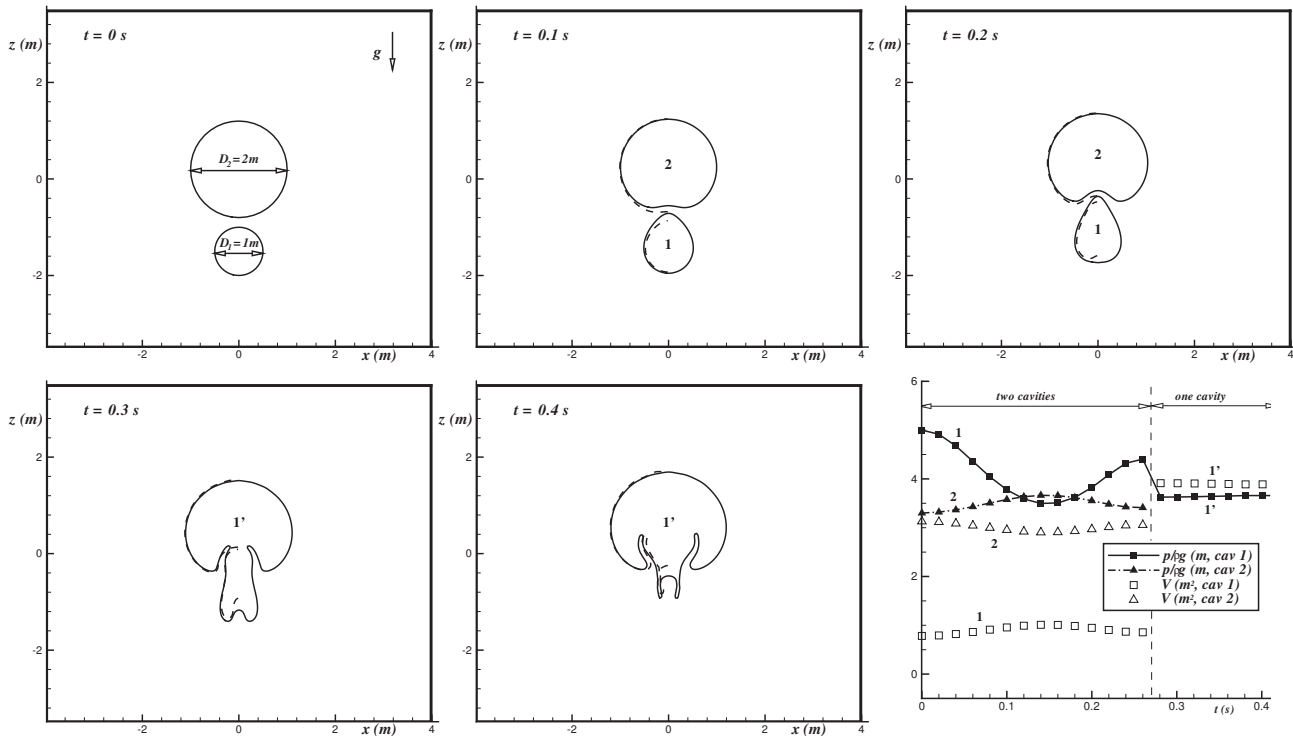


Figure 1: Merging of two cavities. Top-left: initial conditions of the problem in terms of gas-liquid interface and velocity field ( $\mathbf{v} = 0$  everywhere).  $\mathbf{g}$  is the gravity acceleration. For each cavity, the initial pressure has been set equal to the liquid hydrostatic pressure at the center of the cavity. From top-center to bottom-center: evolution of the gas-liquid interface. In each plot, the dashed line is the interface incompressible solution obtained using the NS-LS solver by Colicchio *et al.* (2005). For clarity this has been reported only in the left half-plane. Bottom-right: evolution of the pressure ( $p$ ) and area ( $V$ ) of the cavities. Grid size used for the simulations:  $\Delta x = \Delta z = 0.033D_1$ .

field, while viscous and surface-tension effects are assumed null. Inside each cavity the initial pressure is set equal to the water hydrostatic pressure at the cavity center. This is the initial average bubble pressure predicted when solving the Poisson equation for the incompressible air-water flow. Figure 1 gives the results as evolution of the gas-liquid interface and of the pressures and areas of the cavities. Globally the two cavities start to rise due to the buoyancy and deform as a consequence of the density difference between the two fluids and the compressibility of the air. As time goes on, their pressures tend to become similar and then to diverge, with an oscillatory behavior. At this stage the two bubbles merge and after that evolve in the form of a

single mushroom-shaped bubble. The starting pressure of such bubble is closer to the one inside the largest parent and remains nearly constant in time. Before the merging some compressibility effects are indicated by weak oscillations of the cavities areas ( $V$ ), while later they appear more limited. These aspects are confirmed by the comparison with the incompressible air-water interface results obtained using the NS-LS solver by Colicchio *et al.* (2005). The two solutions are globally close with largest local differences at the initial stages (see figure 1).

The capability of describing the splitting phenomenon is checked by studying the academic problem sketched on the top-left plot of figure 2, where an initially torus air cavity is immersed in a water squared box (side  $L = 4$ ) and is subjected to the action of eight dipoles symmetrically placed along the  $x$  and  $y$  axes. Four of them are at the distance 0.42 from the origin and the others are at the distance 1.18, with strengths equal to 2 and  $-2$ , respectively.

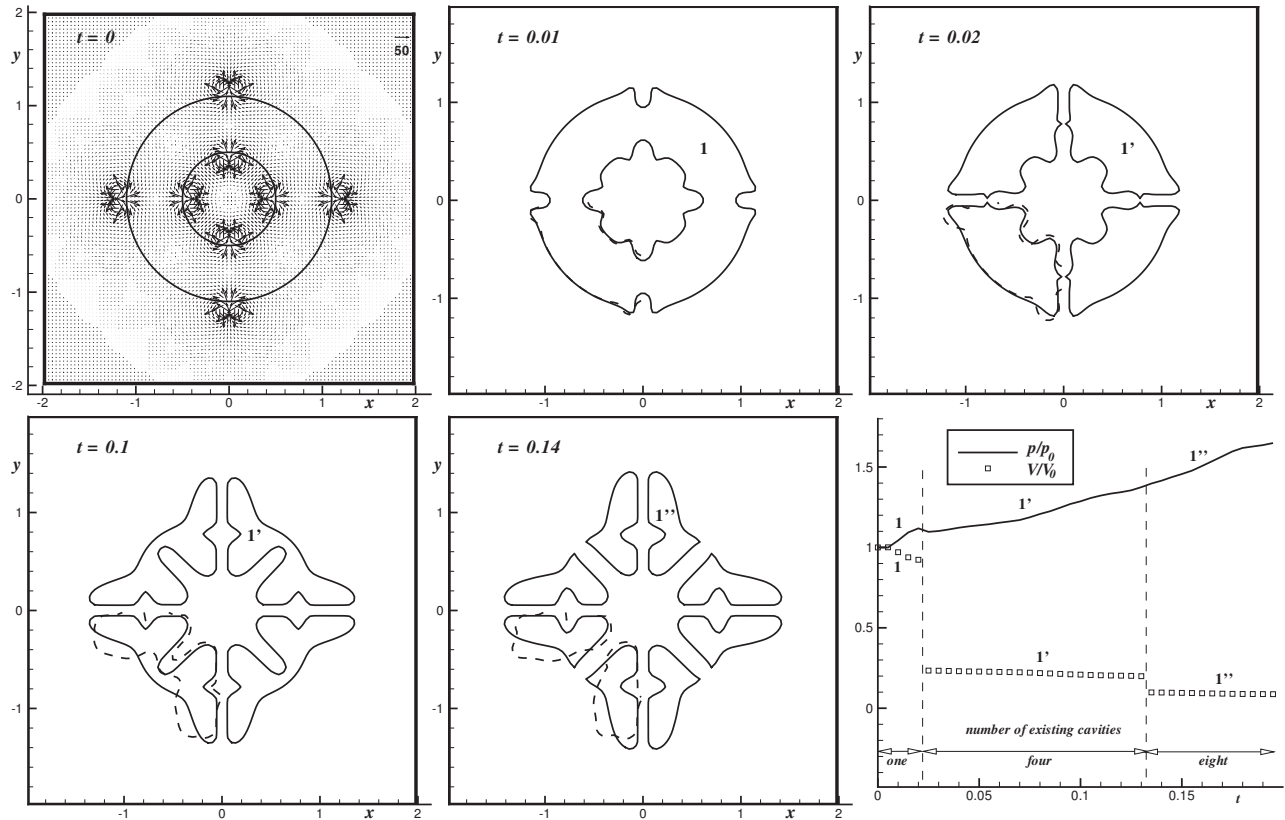


Figure 2: Splitting of a torus cavity subjected to eight dipoles. Top-left: initial conditions of the problem in terms of gas-liquid interface and velocity field. The inner and exterior radius of the initial cavity and its pressure are, respectively,  $r_1 = 0.6$ ,  $r_2 = 0.7$  and  $p_0 = 1$ . From top-center to bottom-center: evolution of the gas-liquid interface. In each plot, the dashed line represents the interface incompressible solution obtained using the NS-LS solver by Colicchio *et al.* (2005). For clarity this has been reported only in the left-bottom quarter. Bottom-right: evolution of the pressure ( $p$ ) and area ( $V$ ) of the developing cavities. For clarity, only the cavities labeled in the evolution plots are considered, because the pressures/areas for the other bubbles follow the same curves given. Grid size used for the simulations:  $\Delta x = \Delta y = 0.067r_1$ .

To keep finite the fluid velocity, the dipoles do not contribute to the local speed in points closer than 1% of the grid size  $\Delta x = \Delta y = 0.04$  from them. The resulting initial velocity field is also shown in the plot. The fluid in this case is viscous but free from gravity and surface tension actions. Figure 2 shows also the time evolution of the air-water interface. The flow caused by the dipoles forces the initial cavity to split in four identical bubbles dividing further in time. The behavior of the pressure  $p$  inside the cavities and the evolution of their areas  $V$  are given in the bottom-right plot of the figure. The area of the initial cavity has a higher change rate than those of the progenies and reduces of about the 10% before the splitting. However the involved time interval is quite limited, so the effects of the initial compressibility in terms of air-water interface deformation become more visible later in the evolution, as confirmed by the comparison with the corresponding incompressible results (see figure 2). To check properly the goodness of the splitting algorithm, this problem has been solved forcing explicitly the symmetries of the velocity and pressure fields. In this way the numerical errors arising when enforcing the symmetries of the examined initial flow on a staggered Cartesian grid have been avoided. The implemented splitting algorithm proved to preserve such symmetries and to correctly evaluate the formation of the new cavities.

The developed compressible solver has been applied to the water shipping problem given in figure 3. The case corresponds to the 2D experiments by Greco *et al.* (2004) and is studied applying the field solver within the domain-decomposition strategy described in Colicchio *et al.* (2006). Compressibility is modeled only inside entrapped cavities and when their size is greater than two grid cells. Bubbles comparable to the grid size, as well as the rest of the air domain, are described as incompressible. In this case viscous effects are considered (but the grid side used is not sufficient to handle the boundary layer along the ship

deck) while the surface tension is not modeled. The incoming waves are generated through a numerical wavemaker moving with the motion of the physical wavemaker measured during the model tests. The water-on-deck caused by their interaction with a barged-shaped ship model starts in the form of a localized plunging hitting the deck. As a result an air cavity is entrapped. Left plot of figure 3 shows a snapshot of the air-water interface after the entrapment and before the collapse in smaller bubbles. The results refer, respectively, to the simulation made assuming everywhere the air incompressible as the water and to the simulations performed modeling the compressibility of the entrapped cavity in the case of model (draft  $D = 0.198$  m) and full (draft  $D = 18$  m) scales.

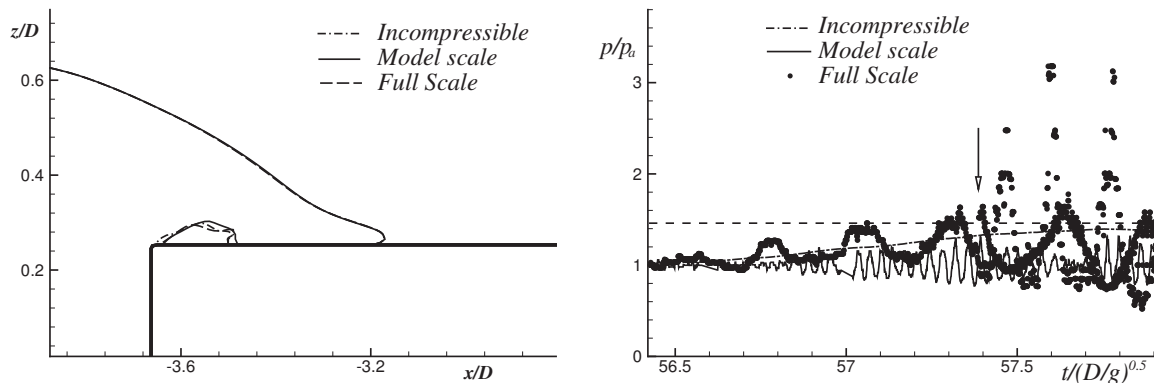


Figure 3: Water-on-deck problem. Left: snapshot of the air-water interface at time  $t = 57.02\sqrt{D/g}$  from the starting of the wavemaker motion. Right: evolution of the pressure inside the entrapped cavities. The grid in the field solver sub-domain is  $dx = dz = 0.01$ .  $D$  is the ship draft, equal to  $D = 0.198$  m at model scale and  $D = 18$  m at full scale, respectively. Grid size used in the NS-LS sub-domain:  $\Delta x = \Delta z = 0.01D$ .

The bubble shapes for the three cases are similar but the full-scale cavity appears closer to the incompressible cavity than to the one predicted at model scale. The full-scale cavity pressure is reported in the right of the same figure and oscillates around the incompressible pressure curve, evaluated as the average pressure inside the cavity. The arrow in the plot shows the time of the first splitting of the full-scale cavity in smaller bubbles (in the considered time interval two cavities are formed), the same symbols as for the initial cavity are used also for the interior pressures of the created bubbles. The pressure at model scale also oscillates but reaches smaller values than at full scale. Further for the considered time interval no splitting phenomenon occurs. The horizontal dashed line in the right plot of figure 3 represents the maximum allowable pressure for the deck of a FPSO ship and is overcome during the time evolution by the pressure inside the full-scale cavity.

A more detailed description of the solution algorithm and of the studies performed with it will be presented at the Workshop.

The present research activity is supported by the Centre for Ships and Ocean Structures (CeSOS), NTNU, Trondheim, within the "Green Water Events and Related Structural Loads" project.

## References

- BARCELLONA, M., M. LANDRINI, M. GRECO, AND O. FALTINSEN (2003). An Experimental Investigation on Bow Water Shipping. *to appear on Journal Ship Research* 47(4).
- CABOUSSAT, A., M. PICASSO, AND J. RAPPAZ (2005). Numerical simulation of free surface incompressible liquid flows surrounded by compressible gas. *J. of Computational Physics* 203, 626–649.
- COLAGROSSI, A. AND M. LANDRINI (2003). Numerical Simulation of Interfacial Flows by Smoothed Particle Hydrodynamics. *Journal of Computational Physics* 191, 448–475.
- COLICCHIO, G. AND M. GRECO (2006). Simplified model for compressible air bubbles in water. In *Proc. of EUROMECH*, Delft, The Netherlands.
- COLICCHIO, G., M. GRECO, AND O. M. FALTINSEN (2006). A BEM-Level Set Domain Decomposition Strategy for Non-linear and Fragmented Interfacial Flows. *J. for Numerical Methods in Engineering*.
- COLICCHIO, G., M. LANDRINI, AND J. CHAPLIN (2005). Level-set Computations of Free Surface Rotational Flows. *Journal of Fluids Engineering, Transactions of the ASME* 127(6), 1111–1121.
- GRECO, M., M. LANDRINI, AND O. M. FALTINSEN (2004). Impact flows and loads on ship-deck structures. *J. of Fluid Mech.* 19(3), 251–275.
- PEREGRINE, D. (2003). Water-wave impact on walls. *Annual Rev. Fluid Mech.* 35, 23–43.
- PEREGRINE, D. AND L. THAUS (1996). The effect of entrained air in violent water waves impact. *Journal of Fluid Mechanics* 325, 377–397.
- RUNGSYAPHORNAT, S., E. KLASEBOER, B. C. KHOO, AND K. S. YEO (2003). The merging of two gaseous bubbles with an application to underwater explosions. *Computers & Fluids* 32, 1049–1079.